

J-integral for delaminated beam and plate models

András Szekrényes

Received 2012-04-30

Abstract

In this work the J -integral is applied to calculate the energy release rate in simple beam and plate models. Four examples are considered: the mode-I double-cantilever beam, the mode-II end-notched flexure, the mixed-mode I/II single-leg bending specimens and a delaminated plate with simply-supported edges, respectively. In each example the details of calculation are given, in the latter case the distribution of the energy release rate along the crack front is calculated. While for delaminated beams the literature presents the energy release rates in numerous studies, the J -integral calculation is not trivial in these cases. Moreover for delaminated bent plates the application of the J -integral is not documented. It is shown that considering the classical plate theory there are serious limitations to calculate representative energy release rates.

Keywords

composite · J -integral · beam theory · plate theory · energy release rate distribution

Acknowledgement

This work was supported by the János Bolyai Research Scholarship of the Hungarian Academy of Sciences and the National Science and Research Fund (OTKA) under Grant No. T34040 (69096). This work is connected to the scientific program of the “Development of quality-oriented and harmonized R+D+I strategy and functional model at BME” project. This project is supported by the New Hungary Development Plan (Project ID: TÁMOP-4.2.1/B-09/1/KMR-2010-0002).

András Szekrényes

Department of Applied Mechanics, BME, H-1111 Budapest, Műegyetem rkp. 5, Hungary
e-mail: szeki@mm.bme.hu

1 Introduction

The J -integral was developed in 1968 by Rice [1] to characterize the strain concentration around cracks and notches. The original definition of the integral is:

$$J = \int_C (Wn_k - \sigma_{ij}u_{i,k}n_j) ds \quad (1)$$

where the parameters will be defined later. Essentially, 2D problems were presented including elastic and elastic-plastic field theories. Later, the method was extended for orthotropic composite materials [2, 3] and 3D problems too [4–6]. In the latter case the so-called J_k vector was defined:

$$J_k = \int_C (Wn_k - \sigma_{ij}u_{i,k}n_j) ds + \int_A (W\delta_{k3} - \sigma_{i3}u_{i,k})_{,3} dA, \quad k = 1, 2 \quad (2)$$

$$J_3 = \int_C (W_3n_1 - \sigma_{3j}u_{3,1}n_j) ds \quad (3)$$

where according to Fig. 1 n_k is the outward normal vector of

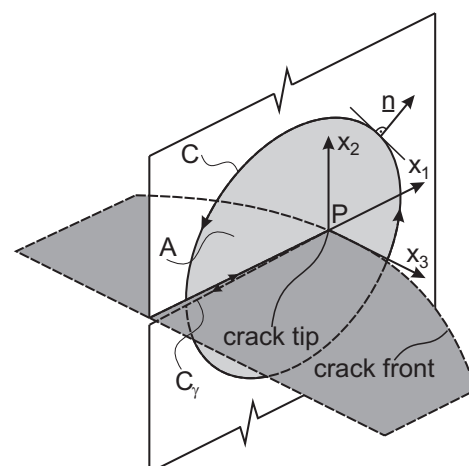


Fig. 1. Reference system for the 3D J -integral.

the contour C , δ_{ij} is the Kronecker tensor, σ_{ij} is the stress tensor ($\sigma_{ij}n_j$ is the traction vector), u_i is the displacement vector, A

is the area enclosed by contour C . The contour C contains the crack tip and the integration is carried out in the counterclockwise direction (see Fig. 1). Under static conditions the J -integral is equivalent to the energy release rate, G , which is also known as the crack driving force [7]. The original brittle fracture model of Griffith [7] applies the

$$G = \frac{\partial U}{\partial A} - \frac{\partial W_F}{\partial A} \quad (4)$$

relation to determine G , which is useful if the dependence of the strain energy, U and work of external forces, W_F are known in the function of crack length a ($dA = bda$, where b is the width). However, for problems, where the mentioned relationships with the crack length are difficult to determine the J -integral is very effective. The energy release rate can be obtained using field theories, i.e. the stress and strain states are to be calculated analytically or numerically. In this paper some basic problems are analyzed, which are in fact simple, but - to telling the truth - not available in the literature and could be useful for those who face to the J -integral application for the first time. Four examples are considered here: the mode-I double-cantilever beam (DCB) [8–16], the mode-II end-notched flexure (ENF) specimen [14, 15, 17, 18] and the mixed-mode I/II single-leg bending (SLB) system [14, 15, 17, 18]. Finally, a simply-supported delaminated elastic plate subjected to a point force is analyzed. In the latter problem a three dimensional analysis is necessary and some nontrivial aspects of the calculation are presented.

2 Example 1. - mode-I double-cantilever beam

The DCB specimen is a very well known, common specimen [11–16], schematically shown in Fig. 2. We analyze two loading schemes: DCB loaded in pure bending and subjected to a point force. Although mainly the second case is involved in practical tests, even the first case has practical importance, see e.g.: [10].

2.1 DCB in pure bending

Fig. 2 shows the DCB subjected to pure bending. The contour consists of four parts. The corresponding stress and displacement components can be obtained by simple beam theory [7]:

$$(1) : \sigma_x = 0, \tau_{xy} = 0, u = 0 \quad (5)$$

$$(2) : \sigma_y = 0, \tau_{xy} = 0, v = \frac{Mx^2}{2IE} \quad (6)$$

$$(3) : \sigma_x = \frac{-12M}{bh^3}y, \tau_{xy} = 0, u = \frac{-12M}{bh^3E}yx \quad (7)$$

$$(4) : \sigma_y = 0, \tau_{xy} = 0, v = \frac{Mx^2}{2IE} \quad (8)$$

where b is the specimen width, h is the thickness, I is the area moment of inertia, E is the flexural modulus. The strain energy density, W is nonzero only for contour No. 3:

$$W = \frac{1}{2}\sigma_x\varepsilon_x = \frac{1}{2}\frac{\sigma_x^2}{E} = \frac{1}{2}\frac{144M^2}{b^2h^6E}y^2 \quad (9)$$

The integral of the strain energy density becomes:

$$\int_C W ds = \int_{h/2}^{-h/2} W dy \Big|_{x=a} = \frac{1}{2}\frac{144M^2}{b^2h^6E}\left[\frac{y^3}{3}\right]_{h/2}^{-h/2} = -\frac{1}{2}\frac{12M^2}{b^2h^3E} \quad (10)$$

where the arc length coordinate is $s = -y$. The second term in the integral is nonzero again only for contour No. 3:

$$\int_C \sigma_{ij}u_{i,k}n_j ds = \int_{h/2}^{-h/2} \sigma_x \frac{du}{dx} ds \Big|_{x=a} = \frac{144M^2}{b^2h^6E}\left[\frac{y^3}{3}\right]_{h/2}^{-h/2} = -\frac{12M^2}{b^2h^3E} \quad (11)$$

The sum of the latter two expressions gives:

$$J_1 = \frac{12M^2}{2b^2h^3E} \quad (12)$$

Considering the fact that we have analyzed only a half model, we have:

$$J_I = 2J_1 = \frac{12M^2}{b^2h^3E} \quad (13)$$

which is well-known from the literature [11–16].

2.2 DCB loaded by concentrated force

The DCB loaded by a wedge force is considered in Fig. 2b. The stress and displacement components for the contour parts based on simple beam theory are:

$$(1) : \sigma_x = 0, \tau_{xy} = 0, u = 0 \quad (14)$$

$$(2) : \sigma_y = 0, \tau_{xy} = 0, v = \frac{P}{2IE}\left(\frac{ax^2}{2} - \frac{x^3}{3}\right) \quad (15)$$

$$(3) : \sigma_x = 0, \tau_{xy} = 0, u = \frac{-P}{bh^3E}\left(ax - \frac{x^2}{2}\right)y \quad (16)$$

$$(4) : \sigma_y = 0, \tau_{xy} = \frac{P}{bh}, v = \frac{P}{2IE}\left(\frac{ax^2}{2} - \frac{x^3}{3}\right) \quad (17)$$

The integral of strain energy density along the through-thickness direction is zero even for contour No. 3:

$$\int_C W ds = \int_{h/2}^{-h/2} W dy \Big|_{x=a} = \frac{1}{2}\int_{h/2}^{-h/2} \tau_{xy}\left(\frac{dv}{dx} + \frac{du}{dy}\right) dy \Big|_{x=a} = 0 \quad (18)$$

which can be explained by the fact that transverse shear deformation is not considered. The second term in Eq. (2) becomes:

$$\int_C \sigma_{ij}u_{i,k}n_j ds = \int_{h/2}^{-h/2} \tau_{xy} \frac{dv}{dx} ds \Big|_{x=a} = -\frac{12P^2a^2}{2b^2h^3E} \quad (19)$$

Again, taking two times the result of the the half model, we have:

$$J_I = 2J_1 = \frac{12P^2a^2}{b^2h^3E} \quad (20)$$

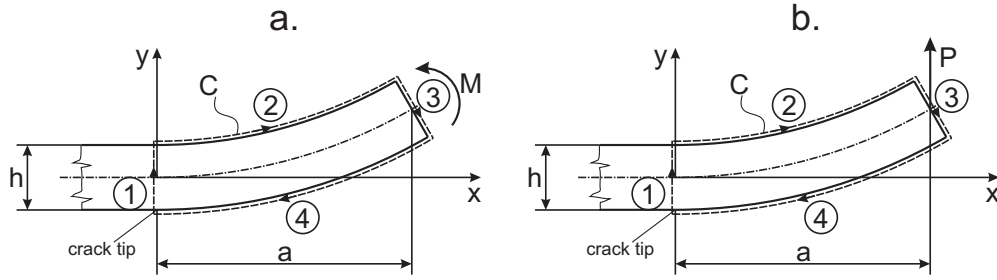


Fig. 2. Double-cantilever beam loaded in pure bending (a) and by a wedge force (b).

3 Example 2. - mode-II end-notched flexure specimen

The ENF specimen is a standard beam for the measurement of the mode-II toughness of composites [14–18]. The specimen geometry is depicted by Fig. 3. For the calculation we define a zero-area path [23] around the crack tip. The dashed lines show the stress and displacement fields on both sides of the tip. The problem is symmetric with respect to the x -axis, therefore we consider the top half of the beam only. The outward normal vectors of contours No. 1 and 2 are:

$$\mathbf{n}_1^T = [1 \ 0 \ 0], \mathbf{n}_2^T = [-1 \ 0 \ 0] \quad (21)$$

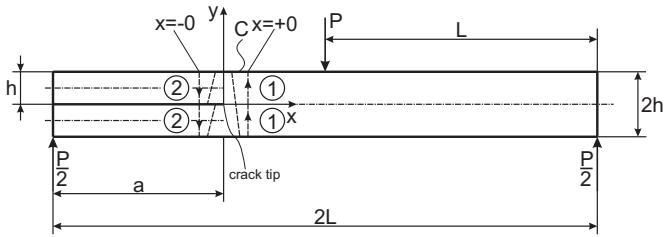


Fig. 3. Integration path for the end-notched flexure specimen.

The stress tensor, traction vector, displacement vector field and its derivative for the right and left contour parts, respectively are:

$$(1) : \boldsymbol{\sigma}_1 = \begin{bmatrix} \sigma_{x1} & 0 & 0 \\ 0 & 0 & 0 \\ 0 & 0 & 0 \end{bmatrix}, \mathbf{T}_1 = \boldsymbol{\sigma}_1 \mathbf{n}_1 = \begin{bmatrix} \sigma_{x1} \\ 0 \\ 0 \end{bmatrix},$$

$$\mathbf{u}_1 = \begin{bmatrix} -v'y \\ v \\ 0 \end{bmatrix}, \frac{d\mathbf{u}_1}{dx} = \begin{bmatrix} -v''y \\ v' \\ 0 \end{bmatrix} \quad (22)$$

$$(2) : \boldsymbol{\sigma}_2 = \begin{bmatrix} -\sigma_{x2} & 0 & 0 \\ 0 & 0 & 0 \\ 0 & 0 & 0 \end{bmatrix}, \mathbf{T}_2 = \boldsymbol{\sigma}_2 \mathbf{n}_2 = \begin{bmatrix} \sigma_{x2} \\ 0 \\ 0 \end{bmatrix},$$

$$\mathbf{u}_2 = \begin{bmatrix} -v'y \\ v \\ 0 \end{bmatrix}, \frac{d\mathbf{u}_2}{dx} = \begin{bmatrix} -v''y \\ v' \\ 0 \end{bmatrix} \quad (23)$$

where $v=v(x)$ the transverse deflection of the beam. The strain energy densities on both sides of the crack tip are given by:

$$W^{(1)} = \frac{1}{2} \sigma_{x1} \varepsilon_{x1} = \frac{1}{2} \frac{\sigma_{x1}^2}{E} = \frac{1}{2} \frac{M_1^2}{I_1^2 E} y^2 \quad (24)$$

$$W^{(2)} = \frac{1}{2} \sigma_{x2} \varepsilon_{x2} = \frac{1}{2} \frac{\sigma_{x2}^2}{E} = \frac{1}{2} \frac{M_2^2}{I_2^2 E} y^2 \quad (25)$$

where $I_1 = bh^3/3$, $I_2 = bh^3/12$ are the area moments of inertia, $M_1 = M_2 = -Pa/4$ are the moments reduced to the crack tip. The integral of strain energy densities in the thickness direction results in:

$$\int_C W ds = \frac{1}{2} \left\{ \int_0^h W^{(1)} dy + \int_{h/2}^{-h/2} W^{(2)} dy \right\} =$$

$$\frac{1}{2} \left\{ \frac{M_1^2}{I_1^2 E} \left[\frac{y^3}{3} \right]_0^h + \frac{M_2^2}{I_2^2 E} \left[\frac{y^3}{3} \right]_{h/2}^{-h/2} \right\} = -\frac{9P^2 a^2}{32b^2 h^3 E} \quad (26)$$

The second part of the J -integral is:

$$\int_C \sigma_{ij} u_{i,k} n_j ds = \int_0^h \mathbf{T}_1 \frac{d\mathbf{u}_1}{dx} dy + \int_{h/2}^{-h/2} \mathbf{T}_2 \frac{d\mathbf{u}_2}{dx} dy =$$

$$\int_0^h \sigma_{x1} (-v''(+0)) y dy + \int_{h/2}^{-h/2} \sigma_{x2} (-v''(-0)) y dy =$$

$$= \int_0^h \frac{M_1}{I_1} \left(\frac{M_1}{I_1 E} \right) y^2 dy + \int_{h/2}^{-h/2} \frac{M_2}{I_2} \left(\frac{M_2}{I_2 E} \right) y^2 dy =$$

$$= \frac{P^2 a^2}{16I_1^2 E} \left[\frac{y^3}{3} \right]_0^h - \frac{P^2 a^2}{16I_2^2 E} \left[\frac{y^3}{3} \right]_{-h/2}^{h/2} = -\frac{9P^2 a^2}{16b^2 h^3 E} \quad (27)$$

The sum of Eqs. (26) and (27) leads to:

$$J_1 = \frac{9P^2 a^2}{32b^2 h^3 E} \quad (28)$$

Taking Eq. (28) two times the energy release rate (ERR) becomes:

$$J_{II} = 2J_1 = \frac{9P^2 a^2}{16b^2 h^3 E} \quad (29)$$

Apparently, this simple formula is well-known in the literature [14, 15, 17, 18].

4 Example 3. - the single-leg bending specimen

As a mixed-mode I/II fracture system we consider the SLB specimen [15, 19–22], shown by Fig. 4. As it is seen, the bottom arm is unloaded. It is reasonable to calculate the mode-I and mode-II ERRs separately. A mode decomposition method has been proposed by Shivakumar and Raju [5] which is based

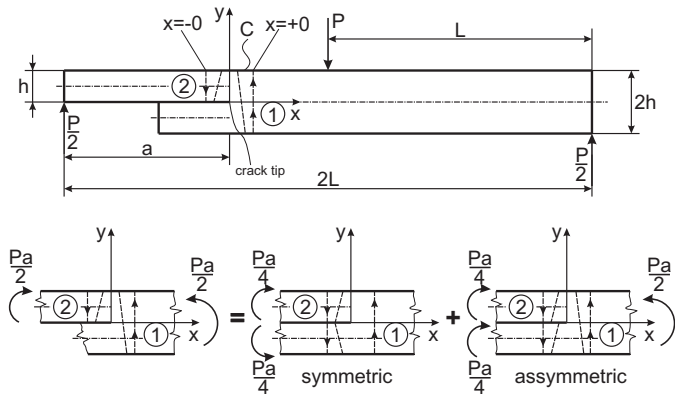


Fig. 4. Integration path and stress decomposition for the single-leg bending specimen.

on the separation of the displacement and stress components into symmetric and antisymmetric parts. Later, it was shown by Rigby and Aliabadi [6] that the stress decomposition in [5] was partly incorrect and the method has been revisited, which was applied later by numerous authors, e.g.: [24, 25]. Fig. 4 shows that in the case of the SLB specimen the stress state can be decomposed by superimposing a DCB loaded by a bending moment $Pa/2$ and an ENF specimen, shown by Fig. 3. For this simple beam problem the method of Shivakumar and Raju [5] is equivalent to the global method by Williams [26]. Thus we have, based on Eqs.(13) and (29) the followings:

$$J_I = \frac{12P^2 a^2}{16b^2 h^3 E}, J_{II} = \frac{9P^2 a^2}{16b^2 h^3 E}, J_{III} = \frac{21P^2 a^2}{16b^2 h^3 E} \quad (30)$$

which has already been published based on strength of materials analysis [15, 19–22].

5 Example 4. - a simply-supported delaminated elastic plate

In this section we present the solution for a simply-supported delaminated plate subjected to a point force. The plate is symmetrically delaminated, hence - since there is no delamination opening - the plate is under mixed-mode II/III fracture condition. Let us consider now Fig. 5, which is the original problem. In fact this problem can be treated as a stepped thickness plate [27, 28] as it is shown by Fig. 5b. Due to the fact that the bending stiffness is piecewise continuous the only alternative is Lévy plate formulation [29–32] to solve the problem.

5.1 Displacement field – Lévy solution

To solve the problem we adopt Lévy plate formulation [29, 32]. The deflection functions and area moments of inertia of the uncracked and delaminated parts are given by:

$$w_1(x, y) : -c \leq x \leq 0, 0 \leq y \leq b, I_1 = \frac{2}{3}t^3 \quad (31)$$

$$w_2(x, y) : 0 \leq x \leq a, 0 \leq y \leq b, I_2 = \frac{1}{6}t^3 \quad (32)$$

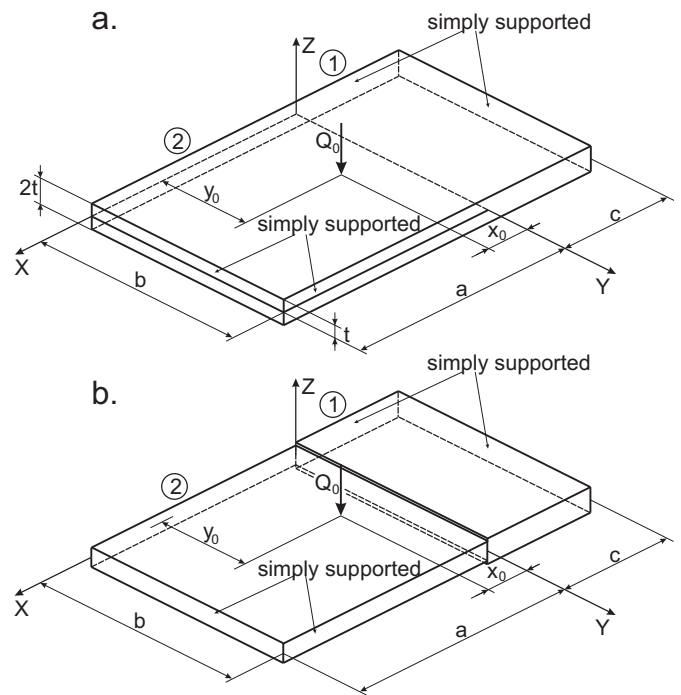


Fig. 5. Delaminated plate subjected to point load (a). Stepped thickness plate (b)

In the y direction the deflections are approximated by \sin functions, i.e. we have:

$$w_1(x, y) = \sum_{n=1}^{\infty} W_{1n}(x) \sin \beta y \quad (33)$$

$$w_2(x, y) = \sum_{n=1}^{\infty} W_{2n}(x) \sin \beta y \quad (34)$$

The governing equation of isotropic, elastic plates is [29]:

$$\frac{\partial^4 w}{\partial x^4} + 2 \frac{\partial^4 w}{\partial x^2 \partial y^2} + \frac{\partial^4 w}{\partial y^4} = \frac{p}{I_1 E_1} \quad (35)$$

where p is the surface pressure and $E_1 = E/(1 - \nu^2)$. Taking Eqs.(31) and (32) back into (39) yields:

$$\frac{\partial^4 W_{1n}}{\partial x^4} - 2\beta^2 \frac{\partial^2 W_{1n}}{\partial x^2} + \beta^4 W_{1n} = 0 \quad (36)$$

$$\frac{\partial^4 W_{2n}}{\partial x^4} - 2\beta^2 \frac{\partial^2 W_{2n}}{\partial x^2} + \beta^4 W_{2n} = \frac{Q_n}{I_2 E_1} \quad (37)$$

where [32]:

$$Q_n = \frac{2Q_0}{b} \delta(x - x_0) \sin \beta y_0 \quad (38)$$

moreover:

$$\delta = \begin{cases} 1 & \text{if } x = x_0 \\ 0 & \text{if } x \neq x_0 \end{cases} \quad (39)$$

The solution functions must satisfy the following boundary conditions:

$$W_{1n}(-c) = 0 \quad (40)$$

$$\frac{\partial^2 W_{1n}}{\partial x^2} - \beta^2 \nu W_{1n} \Big|_{x=-c} = 0 \quad (41)$$

$$W_{2n}(a) = 0 \quad (42)$$

$$\frac{\partial^2 W_{2n}}{\partial x^2} - \beta^2 \nu W_{2n} \Big|_{x=a} = 0 \quad (43)$$

Moreover, continuity of the deflection, slope, bending moment and effective (Kirchhoff) shear force must be ensured involving the following conditions [27, 28]:

$$W_{1n}(0) = W_{2n}(0) \quad (44)$$

$$\frac{\partial W_{1n}}{\partial x} \Big|_{x=0} = \frac{\partial W_{2n}}{\partial x} \Big|_{x=0} \quad (45)$$

$$\begin{aligned} I_1 \left(\frac{\partial^2 W_{1n}}{\partial x^2} - \beta^2 \nu W_{1n} \right) \Big|_{x=0} &= \\ I_2 \left(\frac{\partial^2 W_{2n}}{\partial x^2} - \beta^2 \nu W_{2n} \right) \Big|_{x=0} & \end{aligned} \quad (46)$$

$$\begin{aligned} I_1 \left(\frac{\partial^3 W_{1n}}{\partial x^3} - \beta^2 (2 - \nu) \frac{\partial W_{1n}}{\partial x} \right) \Big|_{x=0} &= \\ I_2 \left(\frac{\partial^3 W_{2n}}{\partial x^3} - \beta^2 (2 - \nu) \frac{\partial W_{2n}}{\partial x} \right) \Big|_{x=0} & \end{aligned} \quad (47)$$

The properties of the analyzed simply supported plate were (refer to Fig. 5): $a = 105$ mm (crack length), $c = 45$ mm (un-cracked length), $b = 100$ mm (plate width), $t = 1.55$ mm (plate thickness), $E = 33$ GPa (modulus of elasticity), $\nu = 0.27$ (Poisson's ratio), $Q_0 = 1000$ N (point force magnitude), $x_0 = 31$ mm, $y_0 = 50$ mm (point of action coordinates of Q_0). The computation was performed by using the code MAPLE [33] by applying 19 Fourier series terms (N) by creating a for-do cycle.

5.2 J -integral evaluation

To calculate the J -integral - similarly to the ENF system - we define a zero-area path around the crack tip in accordance with Fig. 6. The problem is symmetric with respect to the midplane, therefore we analyze only the top half of the plate. The outward normals are given by Eq.(21). This problem involves the 3D J -integral, therefore, Eqs.(2) and (3) must be used. However, due to the zero-area path, the surface integral term in Eq.(2) becomes zero. The stress tensor, traction vector, displacement vector and its derivative for contours No. 1 and 2 are:

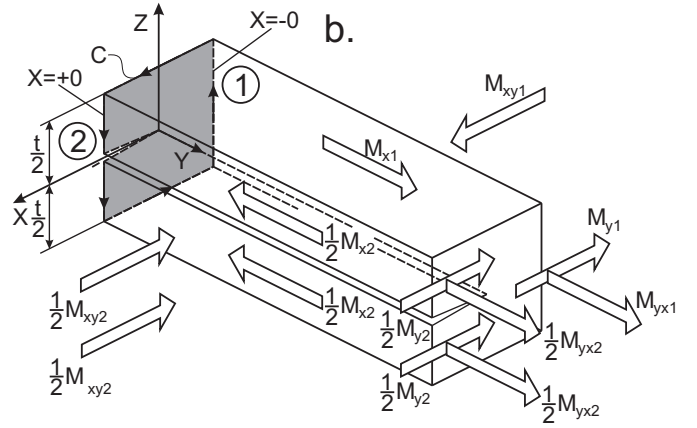


Fig. 6. Integration path and stress couples around the crack tip for an elastic plate.

$$(1) : \sigma_1 = \begin{bmatrix} \sigma_{x1} & \tau_{xy1} & 0 \\ \tau_{yx1} & \sigma_{y1} & 0 \\ 0 & 0 & 0 \end{bmatrix}_{x=0}$$

$$\mathbf{T}_1 = \sigma_1 \mathbf{n}_1 = \begin{bmatrix} \sigma_{x1} \\ \tau_{yx1} \\ 0 \end{bmatrix}_{x=0} \quad (48)$$

$$\mathbf{u}_1 = \begin{bmatrix} -w_{1,x} \cdot z \\ -w_{1,y} \cdot z \\ w_1 \end{bmatrix}_{x=0}, \quad \frac{d\mathbf{u}_1}{dx} = \begin{bmatrix} -w_{1,xx} \cdot z \\ -w_{1,xy} \cdot z \\ w_{1,x} \end{bmatrix}_{x=0}$$

$$(2) : \sigma_2 = \begin{bmatrix} -\sigma_{x2} & -\tau_{xy2} & 0 \\ -\tau_{yx2} & -\sigma_{y2} & 0 \\ 0 & 0 & 0 \end{bmatrix}_{x=+0},$$

$$\mathbf{T}_2 = \sigma_2 \mathbf{n}_2 = \begin{bmatrix} \sigma_{x2} \\ \tau_{yx2} \\ 0 \end{bmatrix}_{x=+0}, \quad (49)$$

$$\mathbf{u}_2 = \begin{bmatrix} -w_{2,x} \cdot z \\ -w_{2,y} \cdot z \\ w_2 \end{bmatrix}_{x=+0}, \quad \frac{d\mathbf{u}_2}{dx} = \begin{bmatrix} -w_{2,xx} \cdot z \\ -w_{2,xy} \cdot z \\ w_{2,x} \end{bmatrix}_{x=+0}$$

Thus, the J_1 integral becomes:

$$\begin{aligned}
 J_1 = & \frac{1}{2} \int_{-h/2}^{h/2} \left\{ \frac{M_{x2}}{I_2} z(-w_{2,xx} \cdot z) + \right. \\
 & \left. \frac{M_{y2}}{I_2} z(-w_{2,yy} \cdot z) + \frac{M_{xy2}}{I_2} z(-2w_{2,xy} \cdot z) \right\}_{x=+0} dz + \\
 & + \frac{1}{2} \int_0^h \left\{ \frac{M_{x1}}{I_1} z(-w_{1,xx} \cdot z) + \right. \\
 & \left. \frac{M_{y1}}{I_1} z(-w_{1,yy} \cdot z) + \frac{M_{xy1}}{I_1} z(-2w_{1,xy} \cdot z) \right\}_{x=-0} dz + \\
 & - \left\{ \int_{-h/2}^{h/2} \left\{ \frac{M_{x2}}{I_2} z(-w_{2,xx} \cdot z) + \frac{M_{yx2}}{I_2} z(-w_{2,xy} \cdot z) \right\}_{x=+0} dz + \right. \\
 & \left. + \int_0^h \left\{ \frac{M_{x1}}{I_1} z(-w_{1,xx} \cdot z) + \frac{M_{yx1}}{I_1} z(-w_{1,xy} \cdot z) \right\}_{x=-0} dz \right\}
 \end{aligned} \quad (50)$$

Since there is no crack opening, we have:

$$J_2 = 0 \quad (51)$$

Finally, J_3 is:

$$\begin{aligned}
 J_3 = & \frac{1}{2} \int_{-h/2}^{h/2} \left\{ \frac{M_{y2}}{I_2} z(-w_{2,yy} \cdot z) + \frac{M_{xy2}}{I_2} z(-2w_{2,xy} \cdot z) \right\}_{x=+0} dz + \\
 & + \frac{1}{2} \int_0^h \left\{ \frac{M_{y1}}{I_1} z(-w_{1,yy} \cdot z) + \frac{M_{xy1}}{I_1} z(-2w_{1,xy} \cdot z) \right\}_{x=-0} dz + \\
 & - \left\{ \int_{-h/2}^{h/2} \left\{ \frac{M_{yx2}}{I_2} z(-w_{2,xy} \cdot z) \right\}_{x=+0} dz + \right. \\
 & \left. \int_0^h \left\{ \frac{M_{yx1}}{I_1} z(-w_{1,xy} \cdot z) \right\}_{x=-0} dz \right\}
 \end{aligned} \quad (52)$$

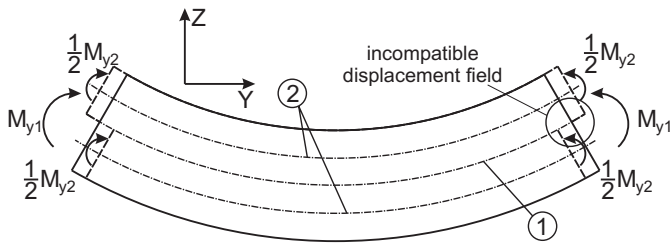


Fig. 7. Incompatible displacement field due to M_y in a delaminated elastic plate.

In Eqs.(50) and (52) the terms related to σ_y and ϵ_y in J_1 and J_3 should be ignored. This can be justified by the incompatible displacement field illustrated in Fig. 7. Theoretically, if there is no crack opening then at the point where the cracked and uncracked parts are connected to each other the strain in the y

direction and the distribution of the stress σ_y are the same, in other words there is no discontinuity between the cracked and uncracked parts. Therefore, in the ideal case the integration of the stress, σ_y produced by the strain in the y direction over the thickness would lead to zero. Consequently, the Kirchhoff plate model predicts erroneously the stress state in the transition zone, which can be counteracted only by ignoring the terms in question. Moreover, in accordance with Fig. 6 it can be seen that M_{xy} is a negative stress couple, while M_{yx} is positive, otherwise they have the same magnitude i.e.: $M_{yx} = -M_{xy}$. It can also be noticed in Fig. 6, that at an actual point they amplify each other. Thus, the J -integrals for the delaminated plate are:

$$\begin{aligned}
 J_1 = & -\frac{1}{2} \left(M_{x2} w_{2,xx} \Big|_{x=+0} - M_{x1} w_{1,xx} \Big|_{x=-0} \right) + \\
 & 2 \left(M_{xy2} w_{2,xy} \Big|_{x=+0} - M_{xy1} w_{1,xy} \Big|_{x=-0} \right)
 \end{aligned} \quad (53)$$

$$J_3 = 2 \left(M_{xy2} w_{2,xy} \Big|_{x=+0} - M_{xy1} w_{1,xy} \Big|_{x=-0} \right) \quad (54)$$

Next, we need to separate J_1 and J_3 into mode-II and mode-III J -integrals. There is a direct decomposition method [5, 6], which provides the mode-I, mode-II and mode-III J -integrals in the form of:

$$J_1 = J_I + J_{II} + J_{III} \quad (55)$$

$$J_2 = -2\sqrt{J_I J_{II}}, J_3 = J_{III} \quad (56)$$

i.e. the J_{III} -integral is directly obtained from J_3 . In our case the mode-I component is zero, thus we have:

$$J_{II} = J_{II}(y) = -\frac{1}{2} \left(M_{x2} w_{2,xx} \Big|_{x=+0} - M_{x1} w_{1,xx} \Big|_{x=-0} \right) \quad (57)$$

$$J_{III} = J_{III}(y) = 2 \left(M_{xy2} w_{2,xy} \Big|_{x=+0} - M_{xy1} w_{1,xy} \Big|_{x=-0} \right) \quad (58)$$

The result of Kirchhoff plate theory is compared to finite element results carried out by ANSYS 12, detailed in next section.

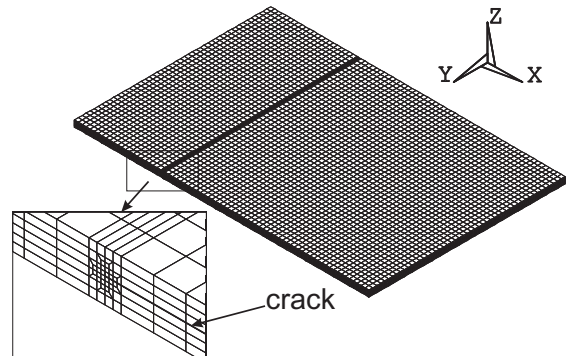


Fig. 8. ANSYS FE model of the simply-supported delaminated plate.

5.3 Numerical solution by VCCT and J -integral

In order to verify the analytical results a finite element analysis was carried out. The 3D finite element model of the plate

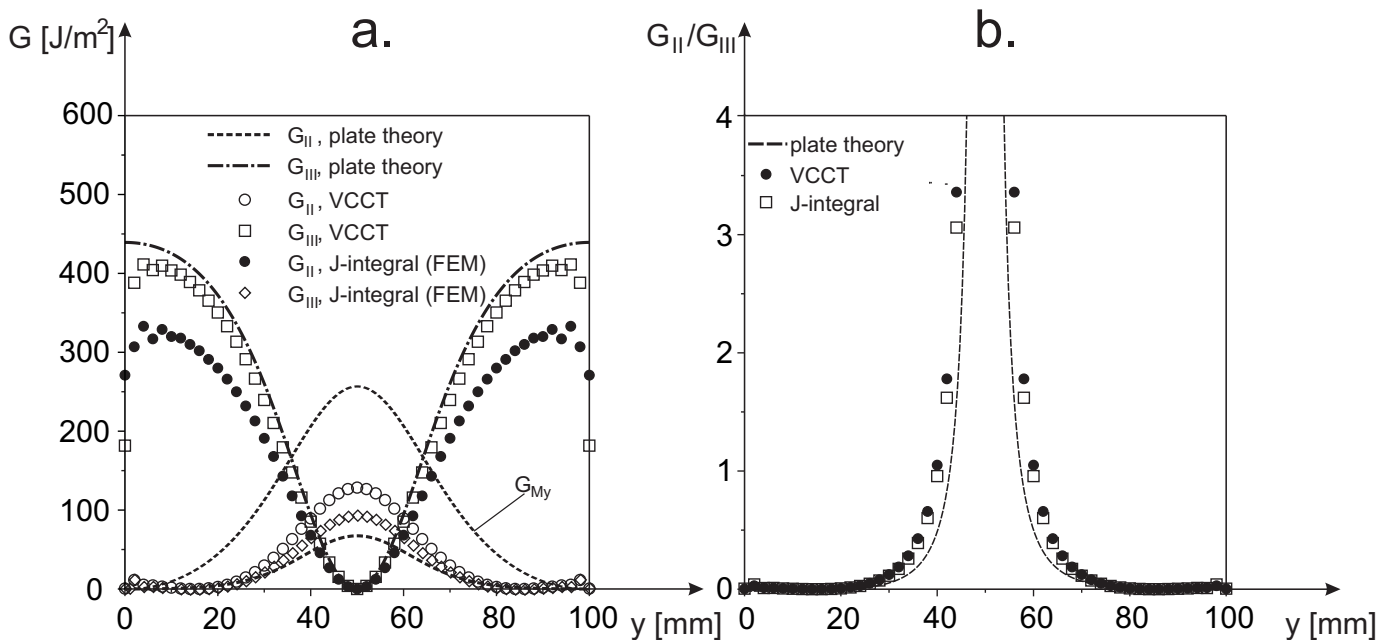


Fig. 9. Energy release rate (a) and mode ratio (b) for an elastic delaminated plate.

is shown by Fig. 8. The model was created in the commercial ANSYS 12 package using 8 node solid elements. In the vicinity of the crack tip a refined mesh was constructed including trapezoid shape elements [19]. The z displacements of contact nodes over the delaminated surface were imposed to be the same. The mode-II and mode-III ERRs were calculated by the virtual crack-closure technique (VCCT, e.g.: [34]), the size of the crack tip elements were $\Delta x = 0.25$ mm, $\Delta y = 0.25$ mm and $\Delta z = 2$ mm. For the determination of G_{II} and G_{III} a so-called MACRO was written in the ANSYS Design and Parametric Language (ADPL). The MACRO gets the nodal forces and displacements at the crack tip and at each pair of nodes, respectively, then by defining the size of crack tip elements it determines and plots the ERRs at each point along the crack front. Apart from the VCCT G_{II} and G_{III} were determined also by the the J -integral, which is available in ANSYS 12 as a built-in command.

5.4 Comparison of analytical and numerical results

The mode-II, mode-III ERRs and the mode ratio along the crack front are shown by Fig. 9. The symbols show the result of the VCCT and the J -integral by FEM, while the curves represent the purely analytical plate theory solutions. It is seen that the mode-II component is significantly underestimated by the plate theory solution. On the contrary the mode-III component is overestimated. While the VCCT predicts that the mode-III ERR decays suddenly near the edges, there is not any decay in accordance with the plate solution. From the practical point of view this difference is insignificant. The crack is expected to initiate/propagate at the points where the highest ERR takes place. This point is in fact almost identical predicted by the two methods. The ANSYS' J -integral underpredicts both ERR components in comparison with the VCCT. In this respect, the plate

theory solution agrees more or less with the mode-II ERR, on the contrary the mode-III component by the numerical J -integral is significantly underpredicted and neither the plate theory nor the VCCT shows good agreement with it. In Fig. 9a the curve marked by G_{My} represents that part of the J -integral, which was calculated by the bending moment M_y and the corresponding strains in the y direction. This curve shows extremely large discrepancy compared to the FE results. This confirms that Kirchhoff plate theory is insufficient in this respect. The mode ratio (G_{II}/G_{III}) is depicted in Figure 9b. It shows that the VCCT and the numerical J -integral is in a reasonably good agreement with each other. The plate theory solution slightly underestimates the mode ratio, however the nature of the curves matches well with the numerical results. The overall agreement between the VCCT and plate theory methods is acceptable. The difference between the VCCT and plate theory solution can be attributed to the transverse and interlaminar shear effects. Further work is necessary to improve the plate theory solution.

Considering the possible application of plate theory solution it must be noted, that nowadays more and more attention is favored to the mode-III and mixed-mode II/III or I/III fracture of composite materials. Recently, de Moraes and Pereira published many studies for carbon/epoxy systems involving the bending of plate specimens. The mode-III 4-point bending plate [35], the mixed-mode I/III 8-point bending [36] and the mixed-mode II/III 6-point bending plate [37] specimens involve the bending of delaminated plates. Analytical reduction techniques are not yet available for these systems. As a future work, by using a proper plate theory this problem is planned to be solved.

6 Conclusions

The application of J -integral has been demonstrated including common fracture specimens and a delaminated simply-

supported isotropic plate. While for cracked beams the J -integral is relatively simple to be calculated, in the plate theory solution some inconsistencies have been elaborated. First, plate have curvatures in the y direction too, and it has been shown that the transition zone between the cracked and uncracked parts are erroneously predicted by the plate model. This can be counteracted by ignoring the stress and displacement components in the y direction when we calculate the J -integral. Second, in the mode-III component it must be considered, that the twisting moments in the different planes amplify each other, consequently in the J -integral their sum appears. Otherwise, based on comparison with finite element calculations plate theory seems to be suitable to calculate energy release rate in delaminated plates, however higher order plate theories may help to achieve better accuracy.

References

- 1 **Rice J R**, *A path independent integral and the approximate analysis of strain concentration by notches and cracks.*, Journal of Applied Mechanics **35** (1968), 379–386, DOI 10.1115/1.3601206.
- 2 **Lee L J, Tu D W**, *J integral for delaminated composite laminates.*, Composites Science and Technology **47** (1993), 185–192, DOI 10.1016/0266-3538(93)90046-J.
- 3 **Valaire BT, Yong YW, Suhling J, Jang B Z, S Q Zhang S Q**, *Application of the J-integral to mixed mode fracture of orthotropic composites*, Engineering Fracture Mechanics **36** (1990), no. 3, 507–514.
- 4 **Murakami T, Sato T**, *Three-dimensional J-integral calculations of part-through surface crack problems*, Computers & Structures **17** (1983), no. 5-6, 731–736, DOI 10.1016/0045-7949(83)90087-1.
- 5 **Shivakumar K N, Raju I S**, *An equivalent domain integral method for three-dimensional mixed-mode fracture problems*, Engineering Fracture Mechanics **42** (1992), no. 6, 935–959, DOI 10.1016/0013-7944(92)90134-Z.
- 6 **Rigby R H, Aliabadi M H**, *Decomposition of the mixed-mode J-integral - revisited*, International Journal of Solids and Structures **35** (1998), no. 17, 2073–2099, DOI 10.1016/S0020-7683(97)00171-6.
- 7 **Anderson T L**, *Fracture Mechanics – Fundamentals and Applications*, CRC Press, Taylor & Francis Group, Boca Raton, London, New York, Singapore, 2005. third edition.
- 8 **Bennati S, Colleluori M, Corigliano D, Valvo P S**, *An enhanced beam-theory model of the asymmetric double cantilever beam (adcb) test for composite laminates*, Composites Science and Technology **69** (2009), no. (11-12), 1735–1745, DOI 10.1016/j.compscitech.2009.01.019.
- 9 **Kenane M, Benmedakhene S, Azari Z**, *Fracture and fatigue study of unidirectional glass/epoxy laminate under different mode of loading*, Fatigue and Fracture of Engineering Materials and Structures **33** (2010), no. 5, 284–293, DOI 10.1111/j.1460-2695.2010.01440.x.
- 10 **Sørensen B F, Jørgensen K, Jacobsen T K, Østergaard R C**, *DCB-specimen loaded with uneven bending moments*, International Journal of Fracture **141** (2006), no. (1-2), 163–176, DOI 10.1007/s10704-006-0071-x.
- 11 **Sorensen L, Botsis J, Gmür T, Humbert L**, *Bridging tractions in mode I delamination: Measurements and simulations*, Composites Science and Technology **68** (2008), 2350–2358, DOI 10.1016/j.compscitech.2007.08.024.
- 12 **Sorensen J, Botsis J, Gmür T, Cugnoni J**, *Delamination detection and characterisation of bridging tractions using long fbg optical sensors*, Composites Part A - Applied Science and Manufacturing **38** (2007), 2087–2096, DOI 10.1016/j.compositesa.2007.07.009.
- 13 **Jumel J, Budzik M K, Shanahan M E R**, *Beam on elastic foundation with anticlastic curvature: Application to analysis of mode I fracture tests*, Engineering Fracture Mechanics **78** (2011), 3253–3269, DOI 10.1016/j.engfracmech.2011.09.014.
- 14 **Yoshihara H, Satoh A**, *Shear and crack tip deformation correction for the double cantilever beam and three-point end-notched flexure specimens for mode I and mode II fracture toughness measurement of wood*, Engineering Fracture Mechanics **76** (2009), no. 3, 335–346, DOI 10.1016/j.engfracmech.2008.10.012.
- 15 **da Silva L F M, Esteves V H C, Chaves F J P**, *Fracture toughness of a structural adhesive under mixed mode loadings*, Materialwissenschaft und Werkstofftechnik **42** (2011), no. 5, 460–470, DOI 10.1002/mawe.201100808.
- 16 **Zhang Y, Vassilopoulos A P, Keller T**, *Mode I and II fracture behavior of adhesively-bonded pultruded composite joints*, Engineering Fracture Mechanics **77** (2010), no. 1, 128–143, DOI 10.1016/j.engfracmech.2009.09.015.
- 17 **Arrese A, Carbajal N, Vargas G, Mujika F**, *A new method for determining mode II r-curve by the end-notched flexure test*, Engineering Fracture Mechanics **77** (2010), no. 1, 51–70, DOI 10.1016/j.engfracmech.2009.09.008.
- 18 **Kutnar A, Kamke F A, Nairn J A, Sernek M**, *Mode II fracture behavior of bonded viscoelastic thermal compressed wood*, Wood and Fiber Science **40** (2008), no. 3, 362–373.
- 19 **Davidson B D, Krüger R, König M**, *Three-dimensional analysis of center-delaminated unidirectional and multidirectional single-leg bending specimens*, Composites Science and Technology **54** (1995), 385–394, DOI 10.1016/0266-3538(95)00069-0.
- 20 **Davidson B D, Bansal A, Bing Q, Sun X**, *Geometrically nonlinear determination of energy release rate and mode ratio in single leg bending tests*, Journal of Reinforced Plastics and Composites **28** (2009), no. 15, 1881–1901, DOI 10.1177/0731684408089235.
- 21 **Davidson B D, Bansal A, Bing Q, Sun X**, *Linear and nonlinear finite element analyses of unidirectional, symmetric single leg four-point bending tests*, Engineering Fracture Mechanics **75** (2008), no. 8, 2130–2143, DOI 10.1016/j.engfracmech.2007.10.009.
- 22 **Oliveira J., Moura M., Morais J.**, *Application of the end loaded split and single-leg bending tests to the mixed-mode fracture characterization of wood*, Holzforschung **63** (2009), no. 5, 597–602, DOI 10.1515/HF.2009.088.
- 23 **Sankar B., Sonik V**, *Pointwise energy release rate in delaminated plates*, AIAA Journal **33** (1995), no. 7, 1312–1318, DOI 10.2514/3.12441.
- 24 **Wearing J., Ahmadi-Brooghani S.**, *The evaluation of stress intensity factors in plate bending problems using the dual boundary element method*, Engineering Analysis with Boundary Elements **23** (1999), 3–19, DOI 10.1016/S0955-7997(98)00057-5.
- 25 **Hamed M., Nosier A, Farrahi G.**, *Separation of delamination modes in composite beams with symmetric delaminations*, Materials and Design **27** (2006), 900–910, DOI 10.1016/j.matdes.2005.03.006.
- 26 **Williams J.**, *On the calculation of energy release rates for cracked laminates*, International Journal of Fracture **36** (1988), 101–119, DOI 10.1007/BF00017790.
- 27 **Guo S.**, *Vibration analysis of stepped thickness plates*, Journal of Sound and Vibration **204** (1997), no. 4, 645–657, DOI 10.1006/jsvi.1997.0955.
- 28 **Yingshi Z**, *Vibrations of stepped rectangular thin plates on Winkler's foundation*, Applied Mathematics and Mechanics (English Edition) **20** (1999), no. 5, 568–578.
- 29 **Timoshenko S, Woinowsky-Krieger S**, *Theory of plates and shells*, McGraw-Hill Book Company, Inc., New York, Toronto, London, 1959. second edition.
- 30 **Ventsel E, Krauthammer T**, *Thin plates and shells - Theory, analysis and applications*, Marcel Dekker, Inc., New York, Basel, 2001.
- 31 **Rudolph S.**, *Theories and applications of plate analysis*, John Wiley & Sons, Inc., Hoboken, New Jersey, 2004.
- 32 **Reddy J.**, *Mechanics of laminated composite plates and shells - Theory and*

- analysis*, CRC Press, Boca Raton, London, New York, Washington D.C., 2004.
- 33 **Garvan F.**, *The Maple Book*, Chapman & Hall/CRC, Boca Raton, London, New York, Washington D.C., 2002.
- 34 **Marat-Mendes R., Freitas M.**, *Failure criteria for mixed mode delamination in glass fibre epoxy composites*, *Composite Structures* **92** (2010), no. 9, 2292–2298, DOI 10.1016/j.compstruct.2009.07.017.
- 35 **Morais A., Pereira A.**, *Mode III interlaminar fracture of carbon/epoxy laminates using a four-point bending plate test*, *Composites Part A - Applied Science and Manufacturing* **40** (2009), no. 11, 1741–1746, DOI 10.1016/j.compositesa.2009.08.009.
- 36 **Pereira A., Morais A.**, *Mixed-mode I + III interlaminar fracture of carbon/epoxy laminates*, *Composites Part A: Applied Science and Manufacturing* **40** (2009), no. 4, 518–523, DOI 10.1016/j.compositesa.2009.02.003.
- 37 **Morais A., Pereira A.**, *Mixed mode II + III interlaminar fracture of carbon/epoxy laminates*, *Composites Science and Technology* **68** (2008), no. 9, 2022–2027.